Electronic Supplementary Information (ESI)

Interfacial Engineering of Rhodium-Complex-Integrated COFs Photocatalysts for Photo-redox Co-factor Cycling and Selective CO_2 Reduction

Shaifali Mishra [a], Rajesh K. Yadav[a], Chandani Singh [b], Rehana Shahin [a], Kanchan Sharma [a], Kamlesh Kumar[d], Mohit[e], Jin OoK Baeg*[b], Joonghan Kim [c]*

[a*]*Department of Chemistry and Environmental Science, Madan Mohan Malaviya University of Technology, Gorakhpur-273010, U.P., India. *E-mail: rajeshkr_yadav2003@yahoo.co.in*

[b*]*Korea Research Institute of Chemical Technology, 141 Gajeong-ro, Yuseong-gu, Daejeon, South Korea. *Email: jobaeg@krict.re.kr*

[c] *Department of Chemistry, The Catholic University of Korea, Bucheon, Gyunggi-do 14662, South Korea, E-mail: joonghankim@catholic.ac.kr*

[d] *Department of Chemistry, Kirori Mal College, University of Delhi, Delhi-110007, India. Email: kamlesh@kmc.du.ac.in*

[e] *Department of Chemistry, University of Delhi (North Campus), Delhi-110007, India. Email: mohit@chemistry.du.ac.in*

Contents

1. General Remarks

Chemicals such as benzene-1,3,5-tricarbaldehyde (Btc), [2,2'-bipyridine]-5,5'-diamine (Bpy), 1,4-dioxane, acetic acid, mesitylene, N, N'-dimethylformamide (DMF), acetone, methanol, diethyl ether, ascorbic acid, sodium mono/dibasic salts, β-NAD^+ co-factor, (pentamethylcyclopentadienyl)-rhodium (III) dichloride dimer and 2,2'-bipyridine were utilized without any purification, sourced from Sigma Aldrich and TCI Chemicals, India. The water used in the reaction medium was distilled, and PBS was prepared from mono/dibasic sodium and potassium salts dissolved in distilled water until a pH of 7 was achieved.

2. Methods and Instrumentation

The characterization was done using different techniques. UV-visible spectroscopy and UV-visible DRS spectroscopy were performed through a Shimadzu UV-1900i spectrophotometer. FTIR analysis was investigated using a Shimadzu 8000 IR spectrometer through KBr pellet support. Electrochemical analysis was performed through a CHI608E-220V instrument, while thermal analysis was examined through an SDT Q600 V20.9 Build 20 instrument with N_2/900 °C (10'C/min, 40ml/min). Powdered X-ray diffraction (XRD) analysis was performed using a Rigaku Smart-Lab High-Resolution X-ray Diffractometer (HRXRD). The X-ray diffraction patterns were recorded in the range of 2θ = 5–70° with Cu Kα radiation (λ = 1.5406 Å) at 45 kV and 200 mA. While the Raman spectroscopy was investigated through the Nano photon Raman force Raman spectrometer. Morphological analysis, like Field-emission scanning electron microscopy (FE-SEM) micrographs, was recorded on a Carl Zeiss Æ©IGMA HD FESEM instrument at 10 keV. The energy dispersive X-ray studies (EDS) were carried out on a Bruker Quantax 200 Energy Dispersive X-ray Spectrometer equipped with a Si Drift Detector (SDD). High-resolution transmission Specific surface area and porosity were determined by N_2 adsorption-desorption isotherms using the Brunauer-Emmett-Teller (BET) method using the Quantachrome Autosorb iQ3. Photoluminescence spectrum measurements were taken by Perkin Elmer LS-55. Electron Microscopy (HR-TEM) images were taken on UC-EF-TEM operated at an accelerating voltage of 200 kV. X-ray photoelectron spectroscopy (XPS) spectra were recorded on an AXIS SUPRA (KRATOS) using a monochromatic Al-Kα X-ray source at 15KeV. ^{1}H NMR spectra were recorded on a Bruker AVANCE II+ 300 MHz spectrometer using tetramethylsilane (TMS, δ = 0) as the internal reference, and formic acid production was analyzed by HPLC using C-18 columns (10 cm

and 25 cm) with a flow rate of 1.5 mL/min, an injection volume of 20 µL with 80% acetonitrile and 20% methanol, and UV detection at 254 nm.

3. Synthesis of Btc-Bpy COFs Films and Post-Synthetic Insertion of Rh Monomer (Btc-Bpy-Rh COFCs)

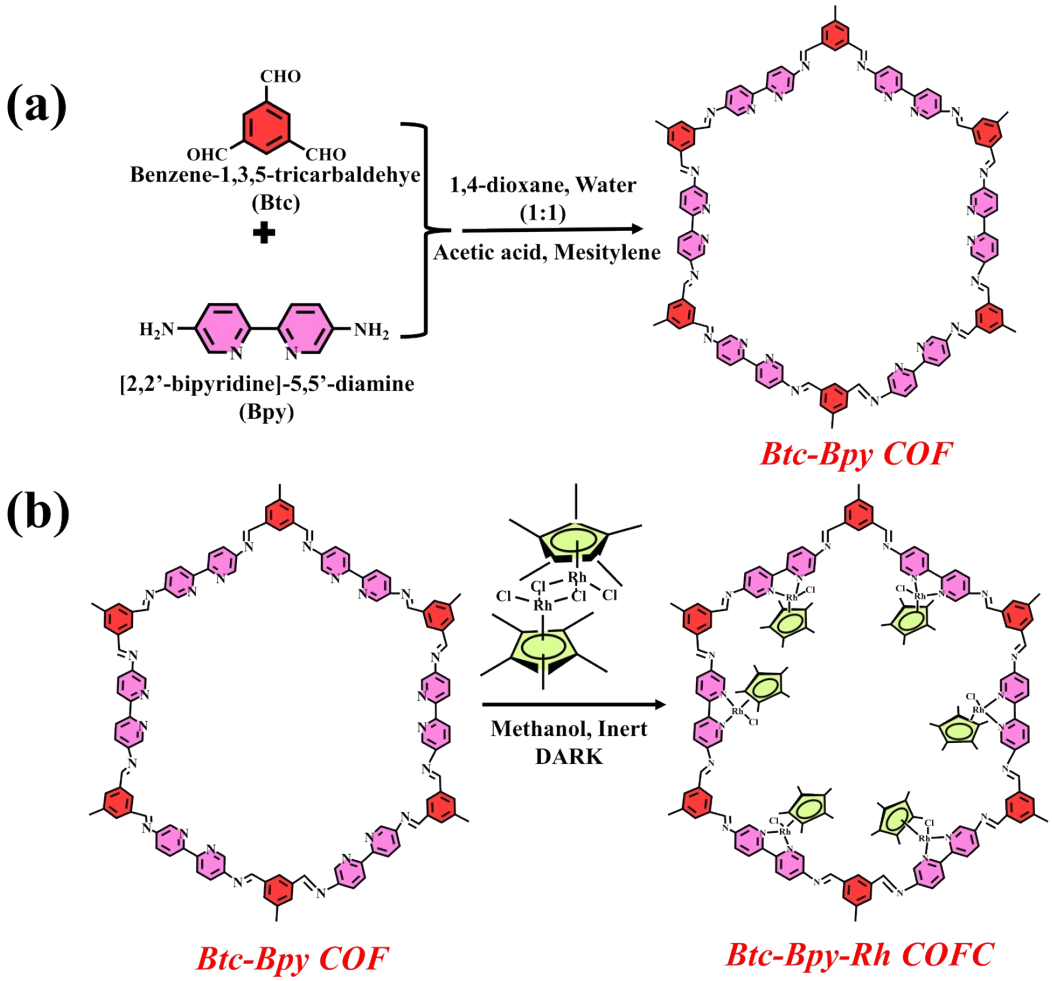

Figure S1: (a) Synthesis of Btc-Bpy COFs, and (b) insertion of Rh monomer to form Btc-Bpy-Rh COFCs.

4. Synthesis of Rhodium complex/Rh-C [RhCp*(bpy)Cl$_2$]

The synthesis of the Rh-C [RhCp*(bpy)Cl$_2$] was carried out following previously reported protocols. Briefly, 25 mg of (pentamethylcyclopentadienyl)rhodium (III) dichloride dimer was dissolved in 5 mL of anhydrous methanol under an inert atmosphere and protected from light. To

this solution, 13 mg of 2,2'-bipyridine (2 equivalents) was added, and the mixture was stirred in the dark. Upon completion of the reaction, diethyl ether was added to induce precipitation. A yellow-coloured solid was formed, collected, and dried under ambient conditions.[1,2]

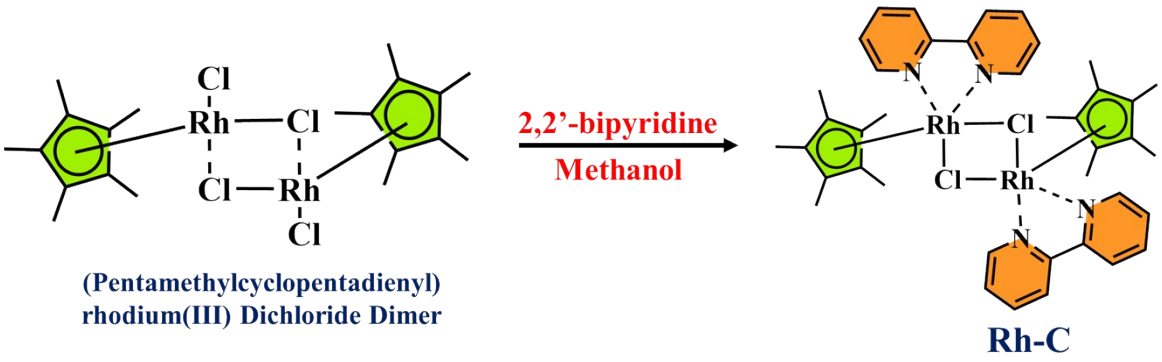

Figure S2: Synthesis of rhodium complex/Rh-C [RhCp*(bpy)Cl_2].

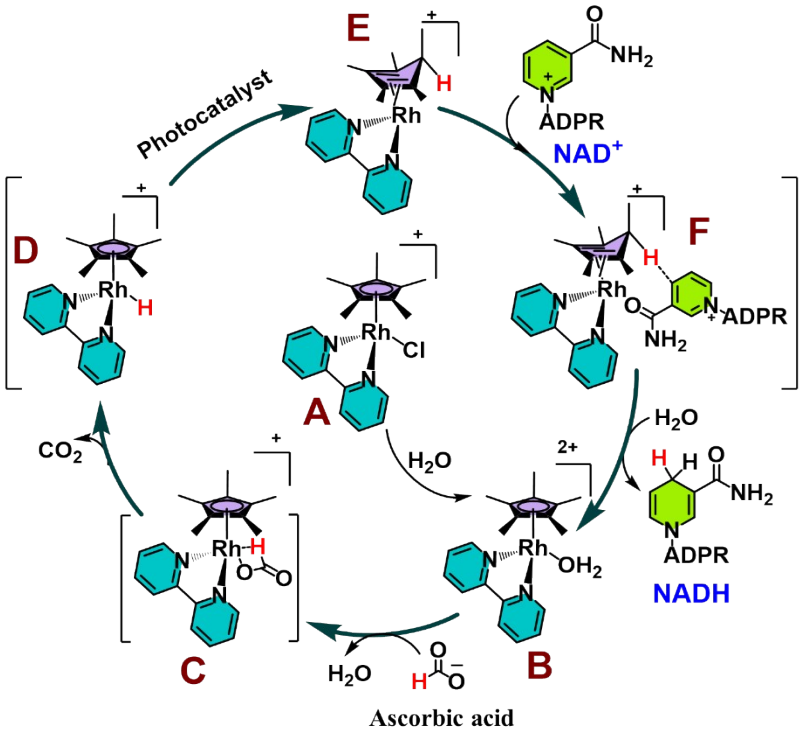

Figure S3: Mechanistic pathway for 1,4-NADH regeneration involving Rh-C.

5. Reusability of Btc-Bpy COFs and Btc-Bpy-Rh COFCs

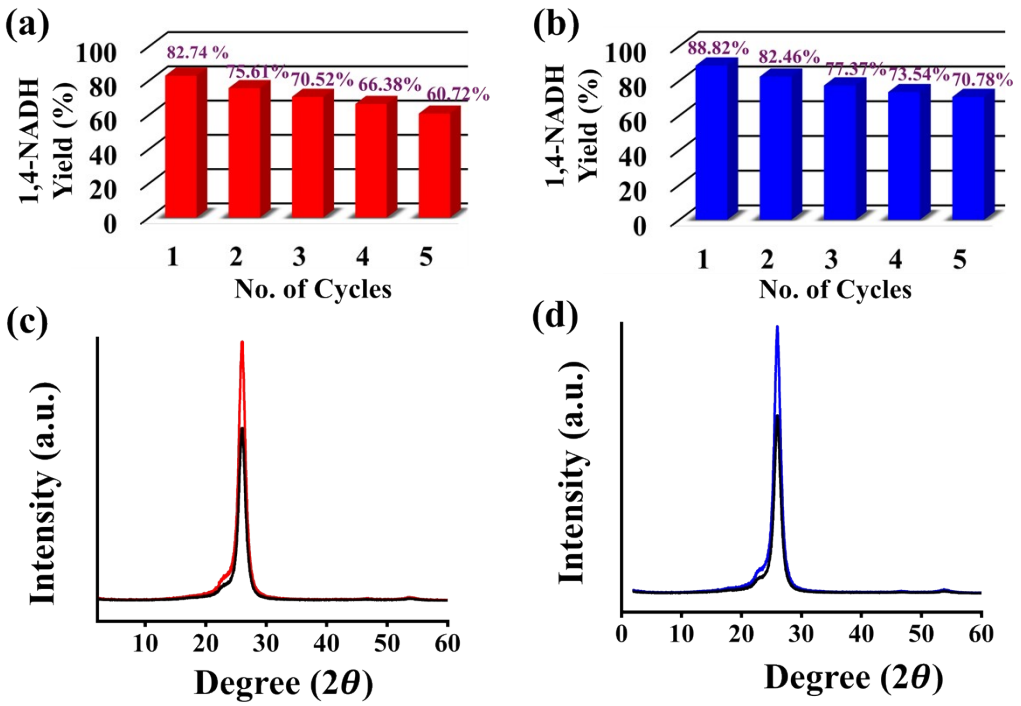

Figure S4: Reusability test for NADH regeneration from (a) Btc-Bpy COFs and (b) Btc-Bpy-Rh COFCs; data represent the average of three independent experiments; error bars correspond to standard deviation (n = 3), and post-PXRD spectra of (a) Btc-Bpy COFs and (b) Btc-Bpy-Rh COFCs.

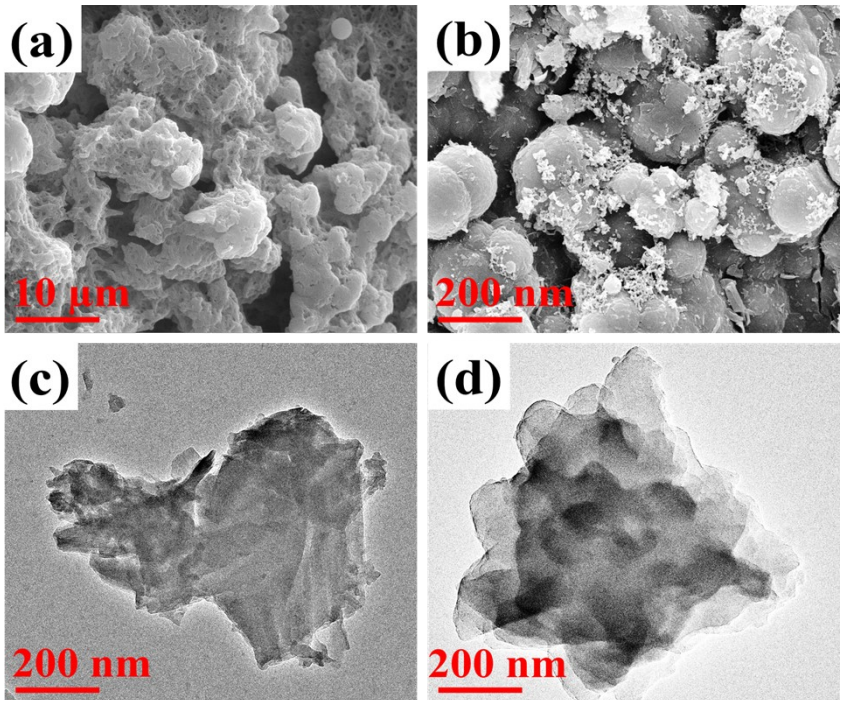

Figure S5: Post micrographs of SEM and TEM of (a,c) Btc-Bpy COFs and (b,d) Btc-Bpy-Rh COFCs.

6. NADH Isomers

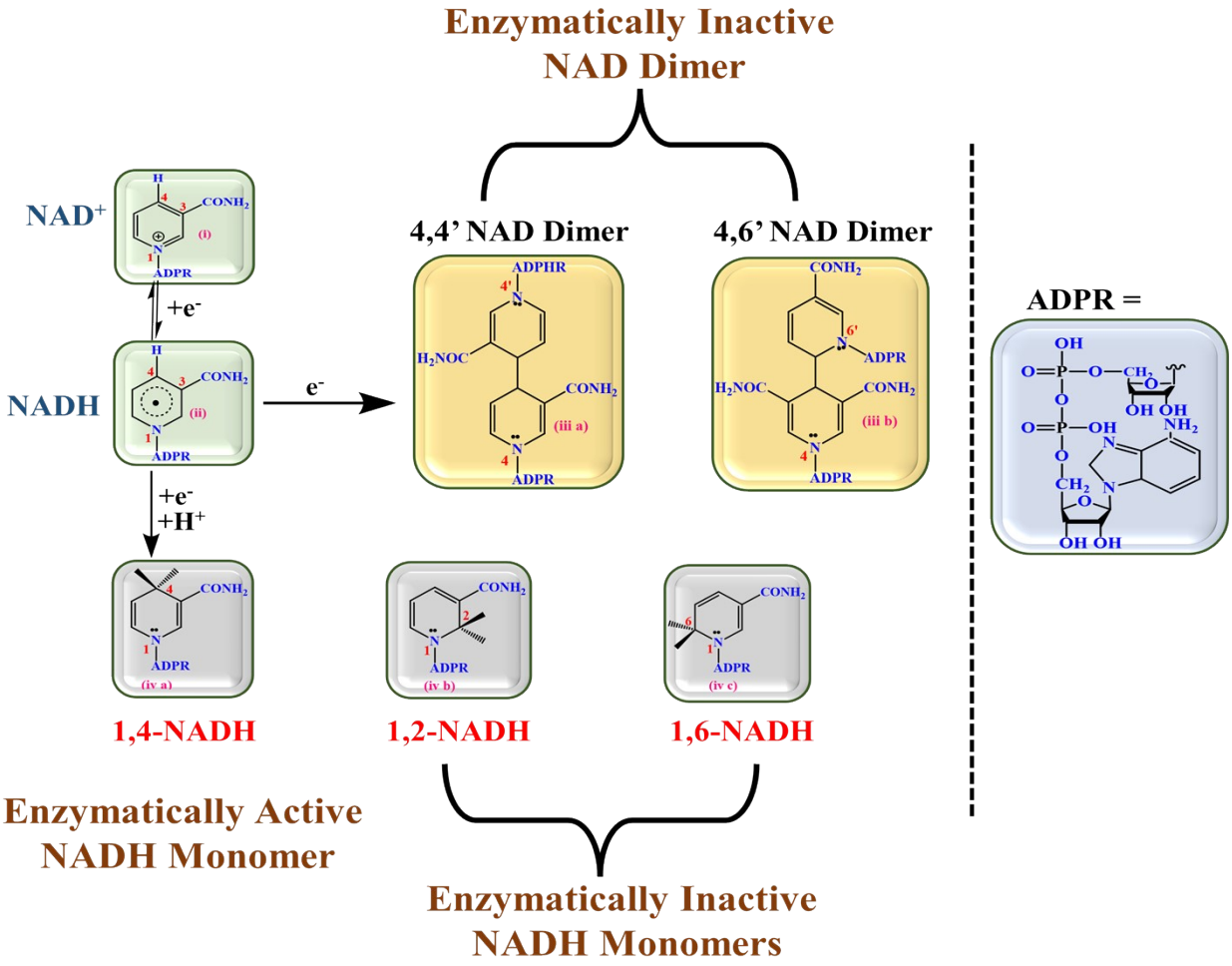

Figure S6: Schematic representation of NADH isomeric forms.

7. Density functional theory (DFT) calculations of Btc-Bpy COFs

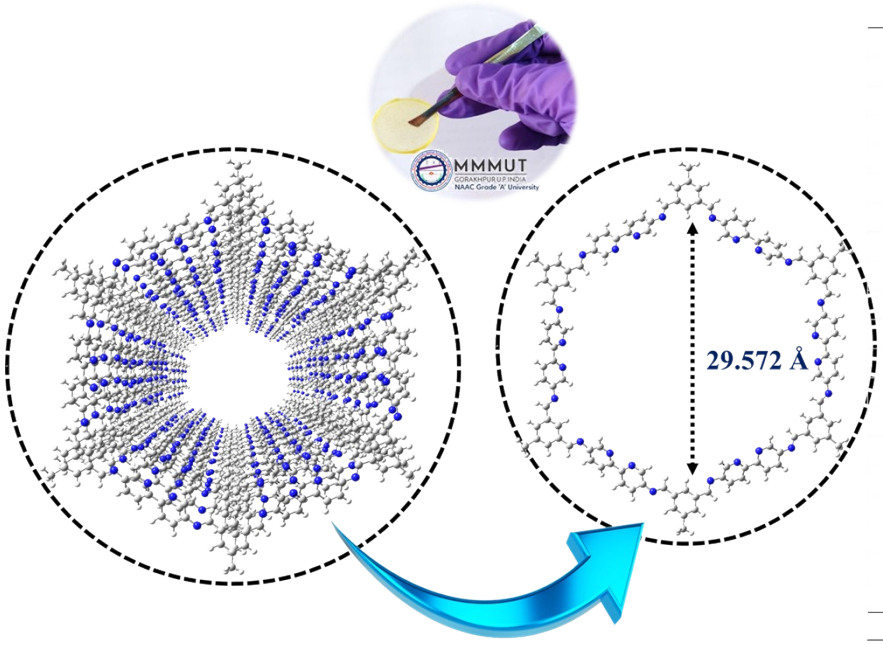

	(eV)
LUMO+9	–2.27
LUMO+8	–2.32
LUMO+7	–2.40
LUMO+6	–2.48
LUMO+5	–2.66
LUMO+4	–2.68
LUMO+3	–2.69
LUMO+2	–2.74
LUMO+1	–2.80
LUMO	–2.87
HOMO	–5.90
HOMO-1	–5.91
HOMO-2	–5.93
HOMO-3	–5.96
HOMO-4	–5.98
HOMO-5	–6.10
HOMO-6	–6.51
HOMO-7	–6.52
HOMO-8	–6.55
HOMO-9	–6.56
E_g	3.03

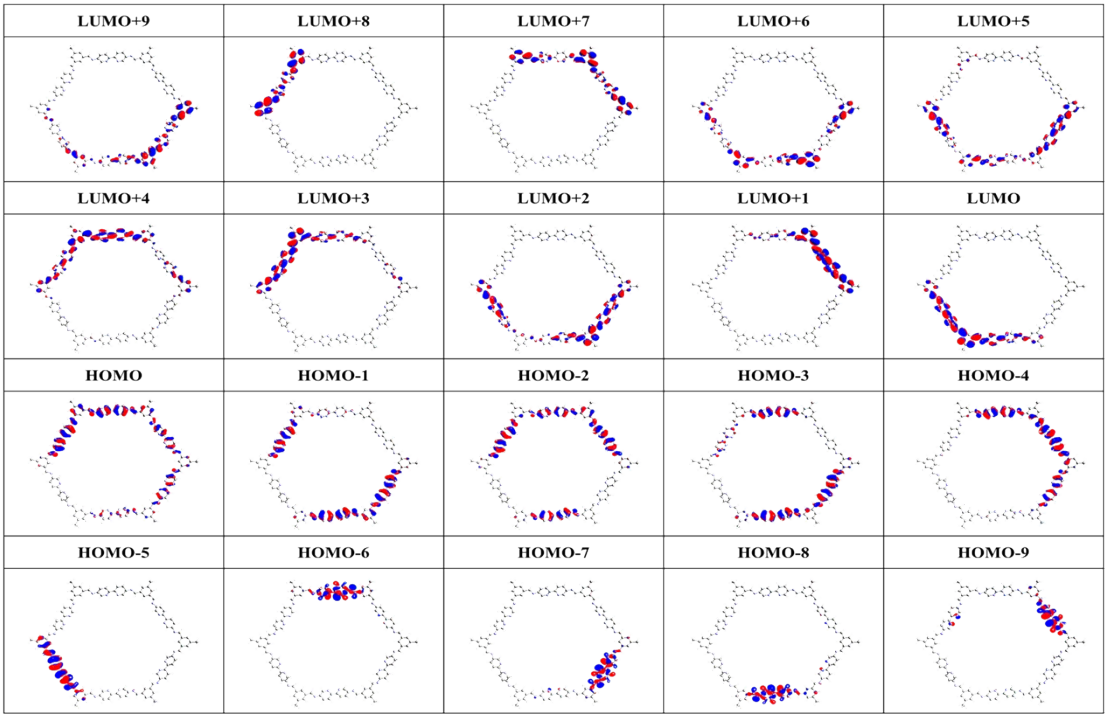

Figure S7: DFT calculations for HOMO/LUMO energy levels.

8. Raman Spectroscopy of Btc-Bpy COFs and Btc-Bpy-Rh COFCs

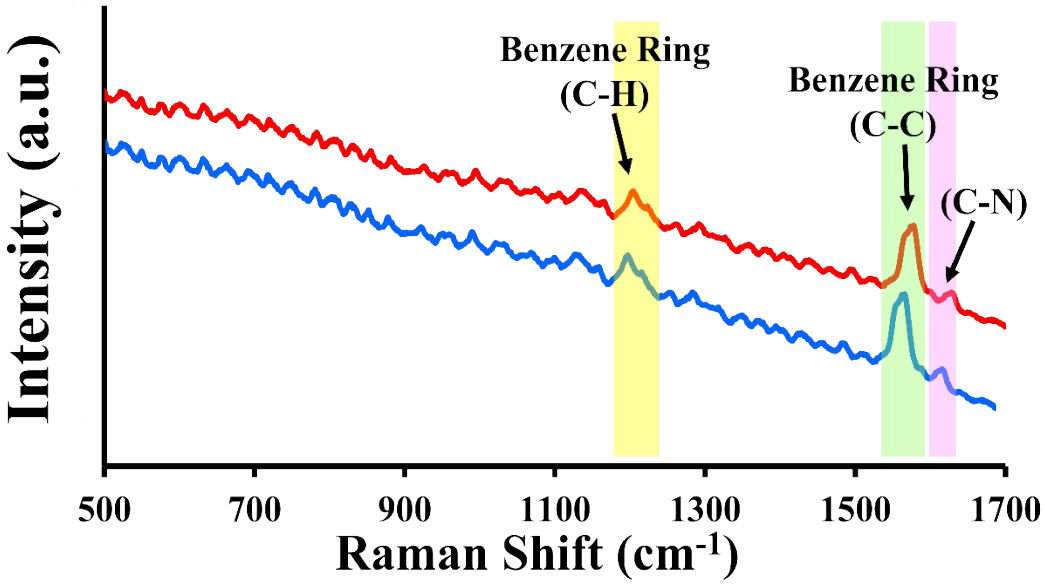

Figure S8: Raman spectra of Btc-Bpy COFs and Btc-Bpy-Rh COFC.[3–5]

9. Thermogravimetric Analysis of Btc-Bpy COFs and Btc-Bpy-Rh COFCs

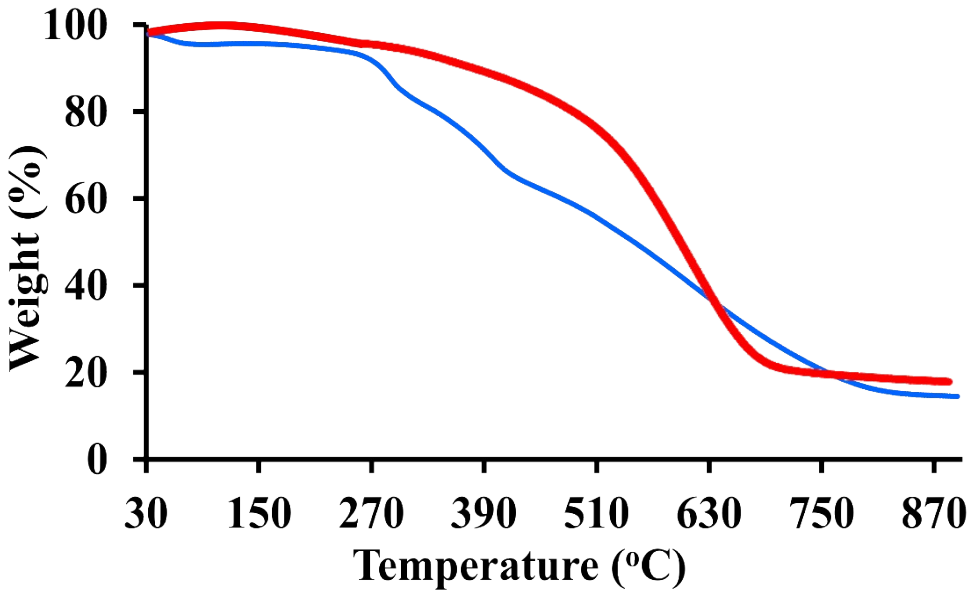

Figure S9: Thermogravimetric analysis (TGA) of Btc-Bpy COFs and Btc-Bpy-Rh COFCs.

10. Cyclic Voltammogram (CV) of Btc-Bpy COFs and Btc-Bpy-Rh COFCs

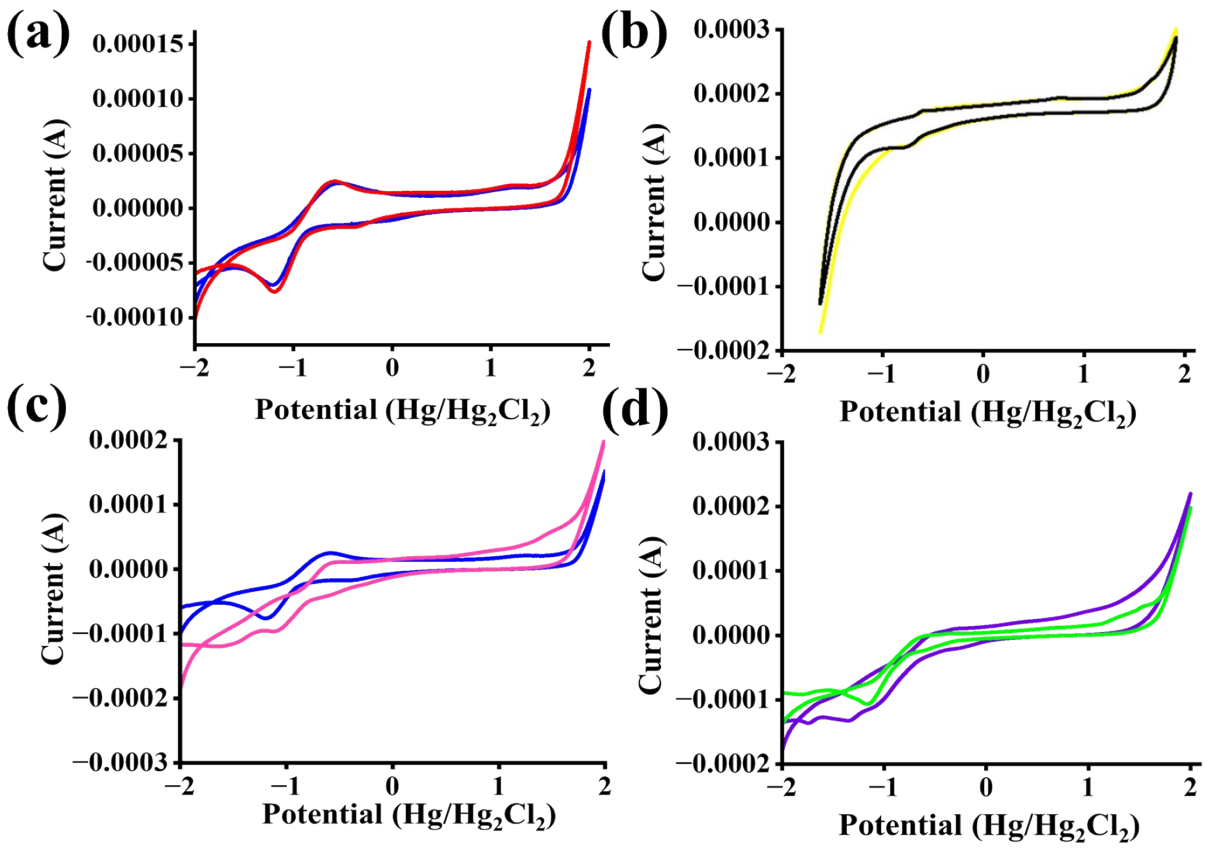

Figure S10: Cyclic voltammogram of (a) Btc-Bpy COFs (red) and Btc-Bpy-Rh COFCs (blue), (b) Rh-C (black) and Rh-C + NAD^+ co-factor (yellow), (c) Btc-Bpy-Rh COFCs (blue) and Btc-Bpy COFs + Rh-C (pink), and (d) Btc-Bpy-Rh COFCs + NAD^+ co-factor (purple) and Btc-Bpy COFs + Rh-C + NAD^+ co-factor (light green).[6]

11. UV-Visible and FTIR spectra of Btc, Bpy as precursors

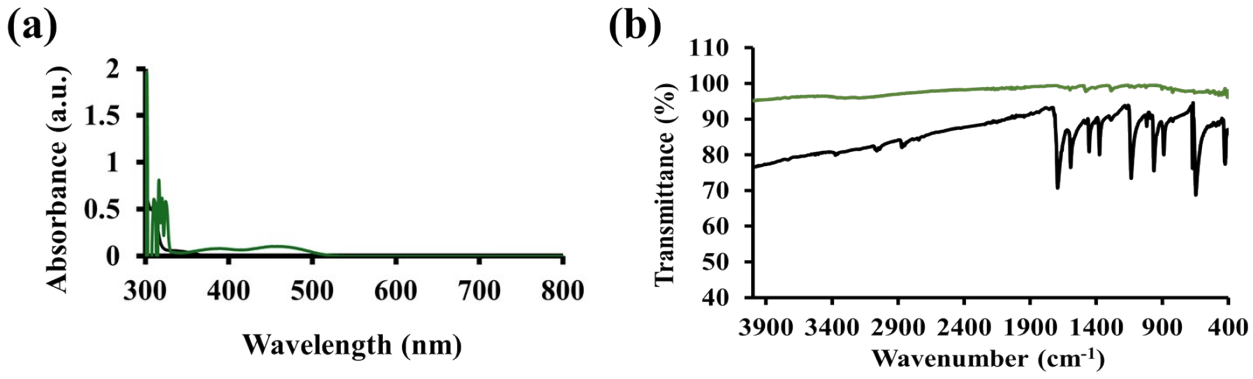

Figure S11: (a) UV-vis. Spectra of Btc (black) and Bpy (green), and FTIR spectra of Btc (black) and Bpy (green).

12. Electrochemical Analysis of Btc, Bpy as precursors

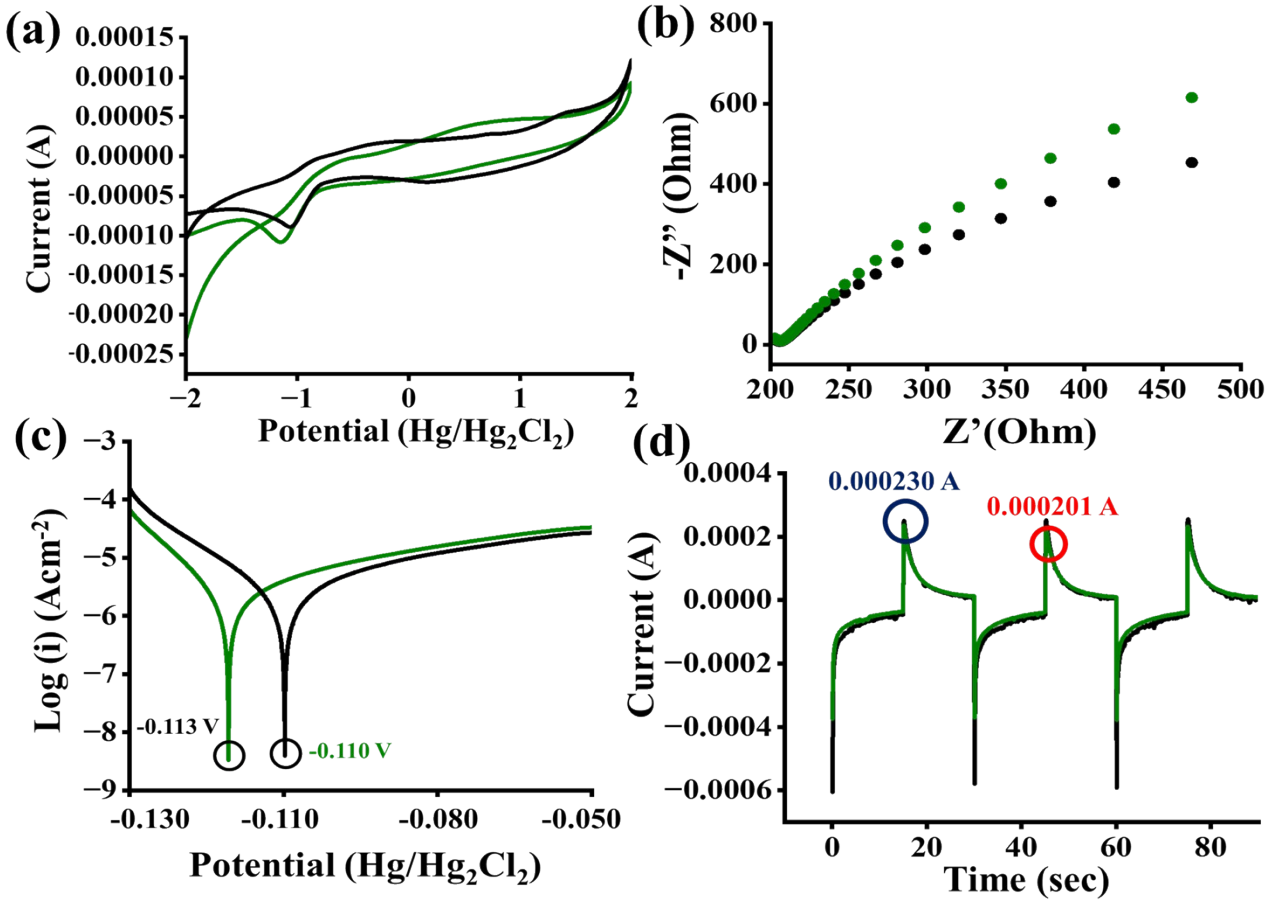

Figure S12: (a) Cyclic voltammogram of Btc (black) and Bpy (green), (b) Electrochemical impedance spectra (EIS) of Btc (black) and Bpy (green), (c) Tafel plot of Btc (black) and Bpy (green), and (d) Chronopotentiometry of Btc (black) and Bpy (green).

13. Quantitative Analysis of 1,4-NADH and Formic Acid

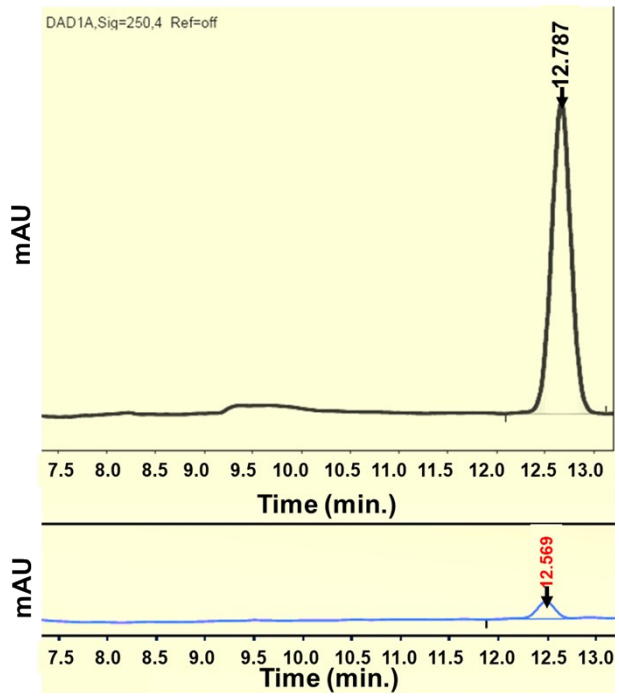

Figure S13: HPLC chromatograms of (a) standard HCOOH, and (b) reaction mixture showing HCOOH formation.

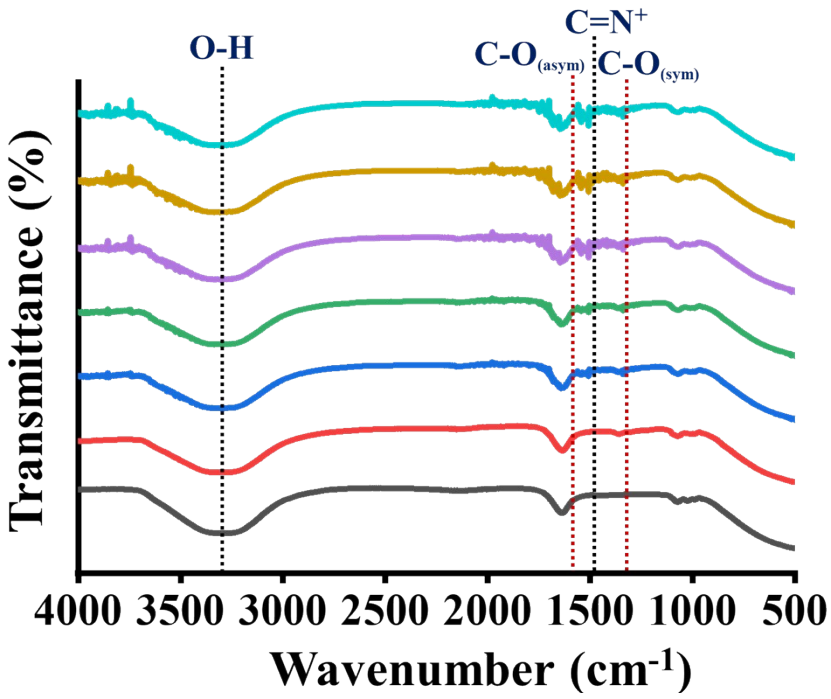

Figure S14: In-situ FTIR of the reaction mixture consisting of formic acid production.

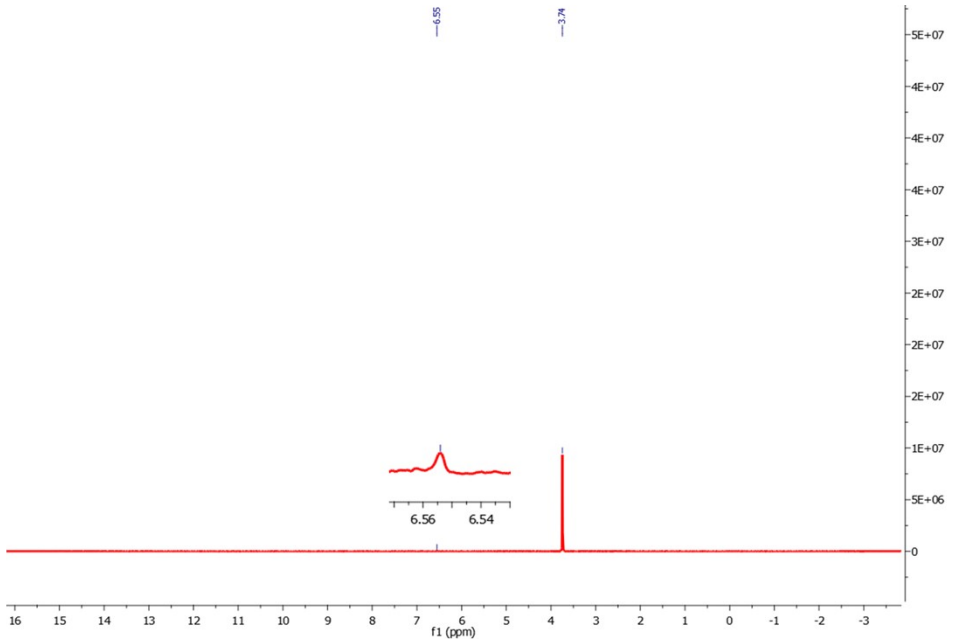

Figure S15: [1]H-NMR spectra of 1,4-NADH (500 MHz, D_2O; δ at 6.55).[7]

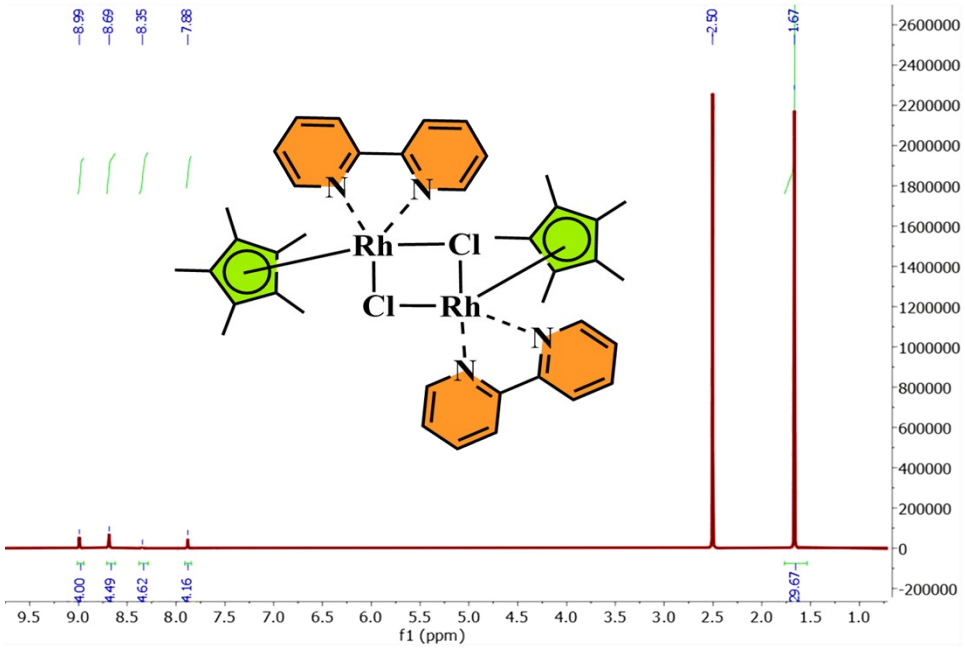

Figure S16: [1]H-NMR spectra of Rh-C [RhCp*(bpy)Cl_2].

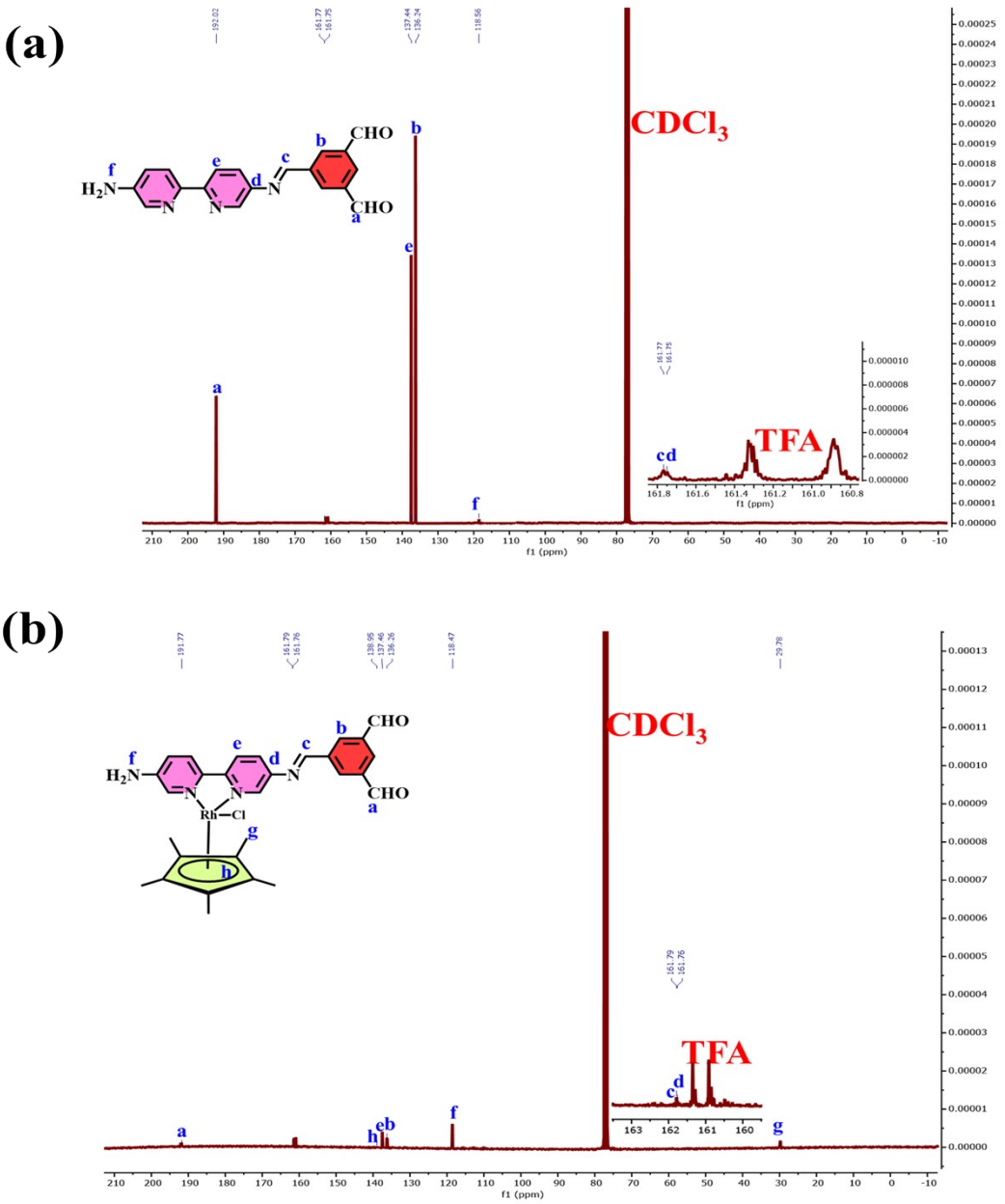

Figure S17: ^{13}C NMR spectra of (a) Btc-Bpy COFs and (b) Btc-Bpy-Rh COFCs, recorded in $CDCl_3$ with trifluoroacetic acid (TFA) as an additive.

S.no.	Photocatalyst	NADH %	Formic acid (mM)	References
1.	UiO67@Rh@UiO66 (COFC)	70.0	-	[8]
2.	CN-CNQD	71.0	-	[9]
3.	Rh-COFBpy@$HCOF_{25}$ (COF)	83.0	-	[10]
4.	PDI/CN	75.0	114.8	[11]
5.	$DDCN_{0.1}$ (Porous Material)	68.0	–	[12]
6.	RF@PANI-2 (Organic Polymer)	70.3	–	[13]
7.	Gold Nanocapsule-FDH Hybrid	22.65	67.40	[14]
8.	Btc-Bpy COFs	82.74	196.93	*This Work*
9.	Btc-Bpy-Rh COFCs	88.82	225.62	*This Work*

Table S1: Comparative summary of catalytic performance parameters of the present system and previously reported catalysts.

S.No.	Derivation from standard conditions	Btc-Bpy COFs	Btc-Bpy-Rh COFCs	Btc-Bpy COFs	Btc-Bpy-Rh COFCs
		NADH (%)		Formic Acid (µM)	
1.	None	82.74	88.82	196.93	225.62
2.	No NAD^+	-	-	-	-
3.	No AsA	-	-	-	-
4.	Dark	-	-	-	-
5.	No FDH	82.74	88.82	-	-
6.	No Rh-C	-	88.82	-	225.62
7.	No Photocatalyst	-	-	-	-
8.	No CO_2	82.74	88.82	-	-

Table S2: Controlled experiments for 1,4-NADH photo-regeneration and formic acid production.

14. References

1 R. K. Yadav, J.-O. Baeg, A. Kumar, K. Kong, G. H. Oh and N.-J. Park, *J. Mater. Chem. A*, 2014, **2**, 5068–5076.

2 S. Mishra, R. K. Yadav, A. Pandey, R. Shahin, N. K. Gupta, D. K. Dwivedi and J. O. Baeg, *Inorg. Chem. Commun.*, 2025, **179**, 114873.

3 A. C. Ferrari, J. C. Meyer, V. Scardaci, C. Casiraghi, M. Lazzeri, F. Mauri, S. Piscanec, D. Jiang, K. S. Novoselov, S. Roth and A. K. Geim, *Phys. Rev. Lett.*, 2006, **97**, 1–4.

4 C. Bathula, I. Rabani, S. Sekar, H. K. Youi, J. Y. Choy, A. Kadam, N. K. Shretha, Y. S. Seo and H. S. Kim, *Ceram. Int.*, 2021, **47**, 8732–8739.

5 C. Zhong, Y. Chen, Y. Zheng, Q. Tian, Y. Chen, M. Xie and Z. Tian, *Anal. Sci.*, 2024, **40**, 1129–1141.

6 R. K. Yadav, J.-O. Baeg, A. Kumar, K. Kong, G. H. Oh and N.-J. Park, *J. Mater. Chem. A*, 2014, **2**, 5068–5076.

7 H. Zheng, Z. Huang, P. Wei, Y. Lin, Y. Cao, X. Zhang, B. Zhou and C. Peng, *ACS Sustain. Chem. Eng.*, DOI:10.1021/acssuschemeng.4c10134.

8 Y. Zhang, B. Wei and H. Liang, *ACS Appl. Mater. \& Interfaces*, 2023, **15**, 3442–3454.

9 Y. Zhou, Y. He, M. Gao, N. Ding, J. Lei and Y. Zhou, *Chinese Chem. Lett.*, 2024, **35**, 108690.

10 H. Zhao, L. Wang, G. Liu, Y. Liu, S. Zhang, L. Wang, X. Zheng, L. Zhou, J. Gao, J. Shi and others, *ACS Catal.*, 2023, **13**, 6619–6629.

11 P. Zhang, J. Hu, Y. Shen, X. Yang, J. Qu, F. Du, W. Sun and C. M. Li, *ACS Appl. Mater. \& Interfaces*, 2021, **13**, 46650–46658.

12 F. Xie, H. Jia, C. K. T. Wun, X. Huang, Y. Chai, C. C. Tsoi, Z. Pan, S. Zhu, K. Ren, T. W. B. Lo and others, *ACS Sustain. Chem. \& Eng.*, 2023, **11**, 11002–11011.

13 L. Zhou, Z. Su, J. Wang, Y. Cai, N. Ding, L. Wang, J. Zhang, Y. Liu and J. Lei, *Appl. Catal. B Environ.*, 2024, **341**, 123290.

14 Y. Wang, M. Gong, H. Wang, G. Xiao, H. Su and J. Xing, *Photocatal. Res. Potential*, 2024, **1**, 10011.